# The N-Terminal Domain of MYO18A Has an ATP-Insensitive Actin-Binding Site†

Yasushi Isogawa,‡ Takahide Kon,‡ Takeshi Inoue,‡ Reiko Ohkura,‡ Hisashi Yamakawa,§ Osamu Ohara,§ and Kazuo Sutoh*,‡

*Department of Life Sciences, Graduate School of Arts and Sciences, University of Tokyo, 3-8-1 Komaba, Tokyo 153-8902, Japan, and Department of Human Gene Research, Kazusa DNA Research Institute, 2-6-7 Kazusa-kamatari, Kisarazu, Chiba 292-0818, Japan*

*Received November 15, 2004; Revised Manuscript Received February 22, 2005*

ABSTRACT: Myosin XVIII is the recently identified 18th class of myosins, and its members are composed of a unique N-terminal domain, a motor domain with an unusual sequence around the ATPase site, one IQ motif, a segmented coiled-coil region for dimerization, and a C-terminal globular tail. To gain insight into the functions of this unique myosin, we characterized its human homologue, MYO18A, focusing on the functional roles of the characteristic N-terminal domain that contains a PDZ module known to mediate protein−protein interaction. GFP-tagged full-length and C-terminally truncated MYO18A molecules that were expressed in HeLa cells exhibited colocalization with actin filaments. Chemical cross-linking of these molecules showed that they form stable dimers as expected from their putative coiled-coil tails. Cosedimentation of the various types of truncated MYO18A constructs with actin filaments indicated the presence of an ATP-insensitive actin-binding site in the N-terminal domain. Further studies on truncated constructs of the N-terminal domain indicated that this actin-binding site is located outside the PDZ module, but within the middle region of this domain, which does not show any homology with the known actin-binding motifs. These results imply that this dimeric myosin might stably cross-link actin filaments by two ATP-insensitive actin-binding sites at the N-terminal domains for higher-order organization of the actin cytoskeleton.

Myosin superfamily proteins, now grouped into 18 classes, play fundamental roles in various cellular functions, including intracellular transport, cellular movements, maintenance of cell shape, and signal transduction (*1*−*3*). A myosin molecule is typically composed of three regions: a motor domain, a neck domain with an IQ motif, and a C-terminal tail. The motor domain is highly conserved among all myosin classes and is responsible for generating directed movement along actin filaments, powered by ATP hydrolysis. The tail domain sequences are very divergent, and contain many different functional motifs that target myosin molecules to specific cellular localizations or mediate interactions with specific proteins. In many cases, the tail domain includes a coiled-coil domain for dimerization (*1*).

Myosin XVIII was recently identified as the 18th class of myosins; it has two subclasses, A and B. Myosin XVIIIA was first isolated from bone marrow stromal cells of mice and designated as MysPDZ (*4*). Myosin XVIIIA has also been found in humans and flies (*4*−*7*). In mice, this myosin is abundantly expressed in stromal cell lines, showing high supportive activity for hematopoietic cell development, though it is also expressed rather ubiquitously in muscle cells and other tissues (*4*).

Myosin XVIIIA has two splice variants, designated as α and *β* in humans and mice. Myosin XVIIIAα is composed of a unique N-terminal domain containing a PDZ[1] module known to act as a scaffold for holding signaling protein complexes together, a motor domain, one IQ motif, a segmented coiled-coil region, and a C-terminal globular tail. Myosin XVIIIA*β* lacks this unique N-terminal domain (*4*, *5*). Myosin XVIIIB has an architecture similar to that of myosin XVIIIA except that the PDZ module in the N-terminal domain is replaced with a stretch of sequence with unknown function (*8*). In addition to the unique N-terminal domain, sequences of motor domains of myosin XVIII subfamily members show several unusual features. First, a flexible loop is inserted at the highly conserved switch 2 region in the ATPase site (Figure 1). Second, the most conserved glutamic acid in the switch 2 region (Figure 1, asterisk) is changed to glutamine in all members of myosin XVIII. This conserved glutamic acid is expected to hold the attacking water for ATP hydrolysis (*9*). Considering that mutation of this strategically critical residue to any other residue abolishes the cellular functions of myosin II in *Dictyostelium* cells (*10*), a glutamine residue in place of glutamic acid might affect the ATPase cycle. Thus, these unusual sequence features of myosin XVIII subfamily members might give rise to unusual consequences in their enzymatic properties. It should be noted that sequence comparison has shown that this subfamily is one of the most

† This work was supported in part by a Grant-in-Aid for Scientific Research (B) from the Ministry of Education, Culture, Sports, Science and Technology, Japan (MEXT), and by a Grant-in-Aid for Scientific Research on Priority Areas from MEXT.

* To whom correspondence should be addressed. Telephone and fax: +81-3-5454-6751. E-mail: sutoh@bio.c.u-tokyo.ac.jp.

‡ University of Tokyo.

§ Kazusa DNA Research Institute.

[1] Abbreviations: GST, glutathione *S*-transferase; GFP, green fluorescent protein; HMM, heavy meromyosin; PBS, phosphate-buffered saline; PDZ, PSD-95/Discs-Large/ZO-1.

10.1021/bi0475931 CCC: $30.25 
Published on Web 03/29/2005

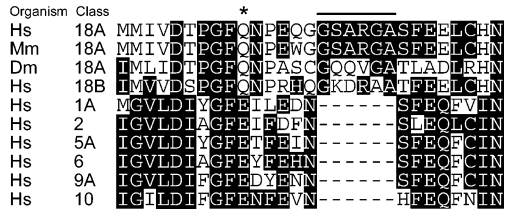


FIGURE 1: Amino acid sequence alignment of the switch 2 region of MYO18A and -B, and other classes of myosin. The bar denotes the unique insertion found only in myosin XVIII. The asterisk denotes the highly conserved glutamic acid, which is converted to glutamine only in myosin XVIII. Gene names and accession numbers are as follows: Hs 18A (MYO18A, D86970), Mm 18A (MysPDZ, AB026497), Dm 18A (Mhcl, AY051503), Hs 18B (MYO18B, AJ310931), Hs 1A (MYO1A, BC059387), Hs 2A (myosin heavy chain IIa, skeletal muscle, adult, AF111784), Hs 5A (MYO5A, U90942), Hs 6 (MYO6, U90236), Hs 9A (MYO9A, AF117888), and Hs 10 (MYO10, AF234532). Hs stands for *Homo sapiens*, Mm for *Mus musculus*, and Dm for *Drosophila melanogaster*.

divergent members of the myosin superfamily (*6*).

It has been reported that the expression level of myosin XVIIIA is correlated with the hematopoietic supportive ability of stromal cells (*4*). Myosin XVIIIA$\beta$ is expressed in all tested hematopoietic cell lines, while myosin XVIIIA$\alpha$ is expressed in only a subset of these cell lines. Furthermore, expression of myosin XVIIIA$\alpha$ is induced upon differentiation of macrophages (*5*). Although these observations might suggest that myosin XVIIIA plays a role in the hematopoietic system, cell biological and biochemical characterizations of this unusual myosin, necessary for understanding its cellular roles, are absent.

To gain some insight into the functions of myosin XVIIIA, we characterized its human homologue, MYO18A, focusing on the functional roles of the unique N-terminal domain, which contains a PDZ module. Using deletion mutants of MYO18A, we found that there is an ATP-insensitive actin-binding site in the N-terminal domain. Further deletion studies showed that this actin-binding site is located outside the PDZ module, indicating that the N-terminal domain characteristic of myosin XVIIIA has two functional modules, an ATP-insensitive actin-binding site and a PDZ module.

## EXPERIMENTAL PROCEDURES

*Expression Constructs.* A pBluescript II SK(+) plasmid (Stratagene, La Jolla, CA) containing human MYO18A cDNA (GenBank accession no. D86970, gene no. KIAA 0216) was obtained from Kazusa DNA Research Institute. A plasmid containing the GCN4 leucine zipper (*11*) sequence (VKQLEDKVEELASKNYHLENEVARLKKLV) was kindly provided by R. D. Vale (University of California, San Francisco, CA).

Synthesized oligonucleotides, 5′-TCGAGTCGACCGGGAATTCTAGACCCGGGCGGCCGCG-3′ and 5′-GATCCGCGGCCGCCCGGGTCTAGAATTCCCGGTCGAC-3′, were annealed with each other and ligated into XhoI−BamHI sites of a pEGFP-C3 vector (BD Biosciences Clontech, Franklin Lakes, NJ) to introduce the NotI sites into its multi cloning site. Synthesized oligonucleotides, 5′-CTAGCGCCACCATGGATCCCGGGTCGACCGGTACCGCGGCCGCCA-3′ and 5′-GATCTGGCGGCCGCGGTACCGGTCGACCCGGGATCCATGGTGGCG-3′, were annealed with each other and ligated into NheI−BamHI sites of a pEGFP-N3 vector (BD Biosciences Clontech) to introduce the BamHI and NotI sites into its multi cloning site. M18A (full-length), HMM, HMM$\Delta$N, ND, and ND-motor (amino acids 4−2054, 1−1349, 334−1349, 1−344, and 4−1190, respectively) were amplified by PCR using human MYO18A cDNA (KIAA 0216) as a template. M18A and ND-motor were subcloned into the modified pEGFP-C3 vector at its BglII and NotI sites. HMM, HMM$\Delta$N, and ND were subcloned into the modified pEGFP-N3 vector at its BamHI and NotI sites. The GCN4 leucine zipper sequence was fused with HMM, HMM$\Delta$N, and ND in their C-terminal NotI sites. MIDDLE-PDZ, PDZ, and MIDDLE (amino acids 108−216, 217−344, and 108−344, respectively) were amplified by PCR and subcloned into pGEX-6P-2 (Amersham Biosciences, Piscataway, NJ) at its BamHI and NotI sites. The GCN4 leucine zipper sequence was fused with MIDDLE-PDZ, PDZ, and MIDDLE in their C-terminal NotI sites.

To amplify MIDDLE-PDZ (RG/AA) and MIDDLE-PDZ (VL/AA) fragments by PCR, synthesized oligonucleotides 5′-GGATCCGGTGAGGAGGGTAGCTTCGCCGCCTCGGTGCTGC-3′ and 5′-GGATCCGGTGAGGAGGGTAGCTTCCGTGGCTCGGCCGCCCAGCGGGCAG-3′ were used as sense primers, respectively, and 5′-CAGAAGAACAGATTGCAGCAGAAGAGGCGGCCGC-3′ was used as an antisense primer. Amplified fragments were subcloned into pGEX-6P-2 at its BamHI and NotI sites. The GCN4 leucine zipper sequence was fused with MIDDLE-PDZ (RG/AA) and MIDDLE-PDZ (VL/AA) in their C-terminal NotI sites.

*Cell Culture and Transfection*. HeLa was obtained from the RIKEN (Ibaragi, Japan) cell bank. HeLa cells were maintained at 37 °C in MEM supplemented with 20 mM glucose and 10% heat-inactivated fetal bovine serum (FBS). Cells were transfected with FuGENE6 (Roche, Basel, Switzerland) according to the manufacturer's protocol.

*Fluorescence Microscopy*. Twelve to fourteen hours after transfection, HeLa cells were fixed with 4% paraformaldehyde in phosphate-buffered saline (PBS) at room temperature for 30 min and permeabilized with 0.2% Triton-X 100 in PBS for 10 min. Permeabilized cells were stained with 6 ng/mL tetramethylrhodamine isothiocyanate-coupled phalloidin (TRITC-Phalloidin, Sigma, St. Louis, MO) in PBS to visualize the actin cytoskeleton. Cells were observed with an LSM510 laser scanning microscope (Carl Zeiss, Oberkochen, Germany).

*Chemical Cross-Linking.* This was performed by using the homobifunctional cross-linking agent bis(sulfosuccinimidyl) suberate ($BS^3$) that was purchased from Pierce (Rockford, IL). Twelve to sixteen hours after transfection, one 60 mm dish of HeLa cells expressing GFP-M18A, HMM-GFP, HMM$\Delta$N-GFP, or GFP-ND-motor constructs were harvested in 0.5 mL of lysis buffer A [20 mM MOPS (pH 7.4), 150 mM NaCl, 1% IGEPAL CA-630 (Sigma), 1 mM EDTA, 1 mM dithiothreitol, and 1 tablet/7 mL of Complete Mini (Roche)] and gently shaken at 4 °C for 1 h. The resulting lysate was centrifuged at 21600*g* for 15 min at 4 °C. The resulting supernatant was mixed with a final concentration of 2 mM $BS^3$, and incubated on ice for 4 min. After incubation, a final concentration of 50 mM Tris was added to quench the cross-linking reaction. The sample was then mixed with an equal volume of phosphate gel sample buffer (56.6 mM $NaH_2PO_4$, 143.6 mM $Na_2HPO_4$, 2% SDS, 8 M

urea, 2% 2-mercaptoethanol, and 0.01% bromophenol blue) and incubated at 37 °C for 2 min. SDS phosphate gels (3.5% acrylamide, 28.3 mM $NaH_2PO_4$, 71.8 mM $Na_2HPO_4$, and 1% SDS) were prepared as described in Sigma technical bulletin MWS-877X. A cross-linked phosphorylase-*b* molecular mass marker (Sigma) was used to calibrate the gels. Samples were resolved by SDS−PAGE using these SDS phosphate gels and the molecular mass marker mentioned above, and then examined by immunoblotting with an anti-GFP antibody (BD Biosciences Clontech).

*Actin Preparation.* Actin was prepared from rabbit skeletal muscle according to the method of Spudich and Watt (*12*), and further purified by gel filtration using a Sephadex G-100 column (Amersham Biosciences). Purified G-actin was polymerized in F buffer [2 mM Tris-HCl (pH 8.0), 50 mM KCl, 2 mM $MgCl_2$, 0.2 mM $CaCl_2$, 0.2 mM ATP, and 0.1 mM dithiothreitol].

*Actin Cosedimentation Assay with Proteins Expressed in HeLa Cells.* Twelve to sixteen hours after transfection, 100 mm dishes (one dish for ND-GFP, two dishes for HMMΔN-GFP, and four dishes for HMM-GFP) of HeLa cells expressing ND-GFP, HMMΔN-GFP, or HMM-GFP constructs were harvested and lysed with sonication in 1.1 mL of lysis buffer B [20 mM MOPS (pH 7.4), 150 mM NaCl, 10 mM $MgCl_2$, 1 mM EGTA, 1 mM dithiothreitol, 0.2 mg/mL soybean trypsin inhibitor, 0.5 mM phenylmethanesulfonyl fluoride, and 1 tablet/7 mL of Complete Mini (Roche)]. The resulting lysate was centrifuged at 436000*g* for 15 min at 4 °C, and the supernatant was mixed with 0.2 mg/mL (a final concentration) actin filaments with or without 0.02 unit/$\mu$L hexokinase (Sigma) and 50 mM glucose (final concentrations). Hexokinase and glucose were added to deplete ATP in the lysates (*13*). Mixed samples were then incubated for 10 min at room temperature. After incubation, a final ATP concentration of 1 mM was added to samples that did not contain hexokinase and glucose to ensure a sufficient amount of ATP in these mixtures. Then all samples were centrifuged at 436000*g* for 10 min at 4 °C. Supernatants were removed and pellets resuspended in an equal volume of PBS. The supernatants and pellets were resolved by SDS−PAGE followed by immunoblotting with an anti-GFP antibody (BD Biosciences Clontech).

*Actin Cosedimentation Assay with GST Fusion Proteins*. GST fusion proteins were expressed in *Escherichia coli* strain BL21 and lysed with sonication in lysis buffer C [10 mM $Na_2HPO_4$, 1.8 mM $KH_2PO_4$ (pH 7.3), 140 mM NaCl, 2.7 mM KCl, 1 mM dithiothreitol, and 1 mM phenylmethanesulfonyl fluoride]. The resulting lysates were centrifuged at 436000*g* for 15 min at 4 °C, and then proteins were purified from the soluble fractions with glutathione−Sepharose 4B (Amersham Biosciences) according to the manufacturer's protocol. Unless otherwise stated, fused GST was removed by cleavage of the recombinant proteins with PreScission protease [40 units per 1 mL of glutathione−Sepharose 4B bed in 50 mM Tris-HCl (pH 7.0), 150 mM NaCl, 1 mM EDTA, and 1 mM dithiothreitol at 4 °C for 4 h]. MIDDLE-PDZ was not cleaved from GST.

The purified proteins were mixed with 0.2 mg/mL (a final concentration) actin filaments and centrifuged at 436000*g* for 10 min at 4 °C. The supernatants were removed and pellets resuspended in an equal volume of PBS. The supernatants and pellets were resolved by SDS−PAGE, and the gels were stained with Coomassie Brilliant Blue.

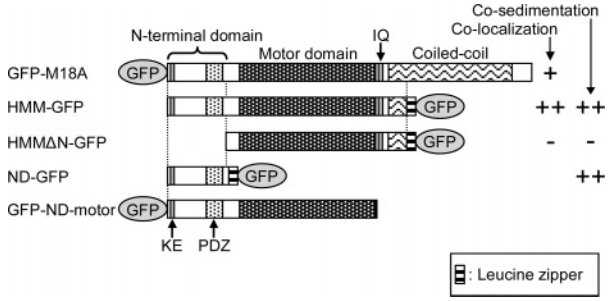


FIGURE 2: Schematic diagram of GFP-tagged full-length and truncated MYO18A constructs expressed in HeLa cells. For colocalization, ++, +, and − represent strong, positive, and no colocalization of the GFP-tagged construct with actin cytoskeletons, respectively. For cosedimentation, ++, +, and − represent strong, positive, and no cosedimentation with actin filaments, respectively.

## RESULTS

*Expression of the Full-Length and C-Terminally Truncated MYO18A Molecules and Their Subcellular Localization.* To gain insight into the cellular functions of MYO18A, we first observed cellular localization of the full-length protein GFP-M18A (Figure 2) constructed by fusing GFP at the N-terminus of MYO18A. GFP was attached at the N-terminus because the tail domain of unconventional myosins often plays a critical role in cellular localization and protein−protein interactions (*14*−*18*). The construct was expressed in HeLa cells, and the transfected cells were fixed to observe GFP fluorescence. GFP-M18A diffusely localized in the cytoplasm, as well as colocalizing with actin filaments (Figure 3A−C), consistent with a previous report (*5*).

To identify the domain responsible for the colocalization of MYO18A with actin, we also expressed a heavy meromyosin (HMM)-like construct, HMM-GFP (Figure 2), which has the truncated coiled-coil tail with 15 heptad repeats followed by a leucine zipper sequence of GCN4 for triggering coiled-coil formation (*19*). GFP was further fused to the C-terminus of GCN4 leucine zipper to visualize the protein in vivo. This HMM-GFP expressed in HeLa cells strongly colocalized with actin filaments with much less diffuse localization in the cytoplasm (Figure 3D−F) compared to the full-length construct. This result indicates that the actin-binding site is not in the C-terminal part of the tail domain deleted to construct this HMM-GFP, but is in the motor domain or in the unique N-terminal domain. However, when the N-terminal domain of HMM was deleted to mimic the myosin XVIIIA$\beta$ variant, the resulting HMMΔN-GFP (Figure 2) did not bind to actin filaments. It was only diffusely distributed in the cytoplasm (Figure 3G−I), consistent with the recent observation that the myosin XVIIIA$\beta$ variant exhibited diffuse localization in the cytoplasm (*5*). These observations imply that a stable actin-binding site is present in the unique N-terminal domain of MYO18A.

*Chemical Cross-Linking of Full-Length GFP-M18A, HMM-GFP, and HMMΔN-GFP.* For further analyses, it needs to be ascertained if GFP-M18A, HMM-GFP, and HMMΔN-GFP form dimers as expected from the coiled-coil structures of their tail regions, since their in vivo localization and affinity with actin filaments might be affected by their higher-

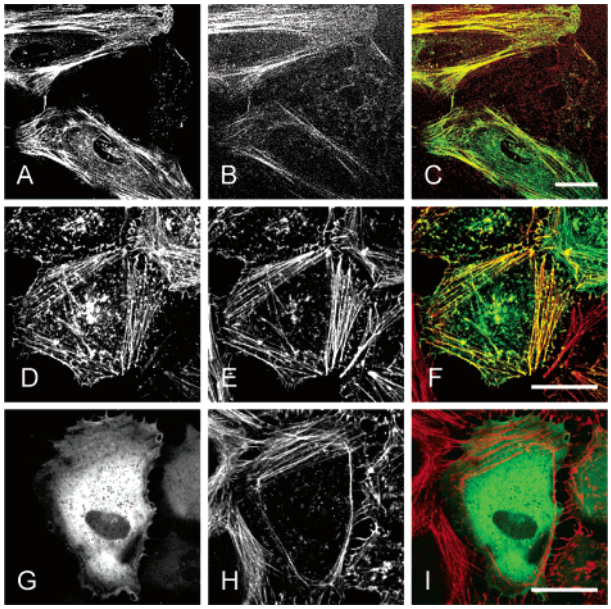


FIGURE 3: N-Terminal domain of MYO18A that is required for cellular colocalization with actin filaments. HeLa cells expressing GFP-tagged MYO18A constructs were fixed and observed by fluorescence microscopy. GFP fluorescence shows localization of the MYO18A constructs (A, D, and G). Actin filaments are visualized with TRITC-phalloidin (B, E, and H). Corresponding overlaid images are also shown (C, F, and I). (A−C) Full-length GFP-M18A localizes diffusedly in the cytoplasm and also colocalizes with actin filaments. (D−F) HMM-GFP strongly colocalizes with actin filaments. (G−I) HMMΔN-GFP localizes diffusedly only in the cytoplasm but not to actin filaments. Bars are 10 $\mu$m long.

order structures. It has recently been shown that myosin VI with a putative coiled-coil structure at its tail is present as a monomeric protein in vivo (*20*). Chemical cross-linking with $BS^3$ [bis(sulfosuccinimidyl) suberate], which has an arm length of 11.4 Å and cross-links with two side chains of lysine residues, was performed on the lysate of HeLa cells expressing GFP-M18A, HMM-GFP, or HMMΔN-GFP. SDS−PAGE of cross-linked products and visualization of these polypeptide chains with an anti-GFP antibody showed that these molecules easily formed cross-linked dimers (Figure 4). Under the same cross-linking conditions, monomeric GFP-ND-motor molecules (Figure 2), which completely lost their coiled-coil tail, were not cross-linked (Figure 4). The experiments indicate that full-length MYO18A and its truncated derivatives with coiled-coil tails are actually present as dimers.

*Cosedimentation with Actin Filaments.* We then performed actin cosedimentation with HMM-GFP or HMMΔN-GFP in the lysate of HeLa cells expressing these proteins. As shown in Figure 5, HMM-GFP cosedimented well with actin filaments added to cell lysates both in the presence of 1 mM ATP and in the presence of an excess amount of hexokinase and glucose to deplete ATP in the cell lysates (see Experimental Procedures). Unlike HMM-GFP, HMMΔN-GFP did not cosediment with actin filaments in the presence of ATP or in the presence of hexokinase and glucose (Figure 5); thus, it is very likely that the stable ATP-insensitive actin-binding site is not in the MYO18A motor domain, but in the N-terminal domain. This notion was further confirmed by performing actin cosedimentation with a construct containing the N-terminal domain alone. This N-terminal domain construct fused with the GCN4 leucine zipper and GFP at its C-terminus (designated as ND-GFP, Figure 2) cosedimented with actin filaments irrespective of ATP concentration (Figure 5).

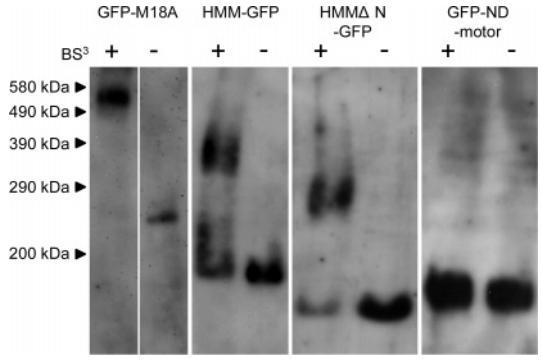


FIGURE 4: Chemical cross-linking of GFP-M18A, HMM-GFP, HMMΔN-GFP, and GFP-ND-motor. HeLa cells expressing each construct were lysed. After centrifugation, the supernatant was incubated on ice with 2 mM $BS^3$ for 4 min. Controls without $BS^3$ were left on ice for 4 min. Samples were subjected to 3.5% acrylamide SDS−PAGE gels and detected by Western blotting using an anti-GFP antibody. Molecular mass markers (kilodaltons) are given at the left. Predicted molecular masses are as follows: 260 kDa for GFP-M18A, 180 kDa for HMM-GFP, 140 kDa for HMMΔN-GFP, and 160 kDa for GFP-ND-motor.

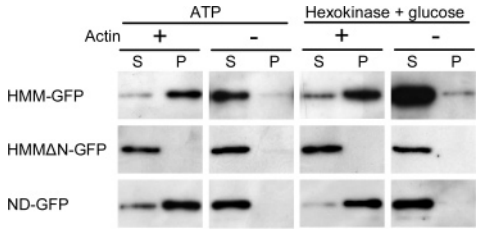


FIGURE 5: N-Terminal domain contains an ATP-insensitive actin-binding site(s). High-speed supernatants were obtained from HeLa cells expressing MYO18A constructs. The supernatants were mixed with (+) or without (−) actin filaments in the presence of 1 mM ATP or in the presence of 0.02 unit/$\mu$L hexokinase and 50 mM glucose to deplete ATP. The samples were then centrifuged at 436000*g*. Resulting supernatants (S) and pellets (P) were subjected to SDS−PAGE and detected by Western blotting using an anti-GFP antibody. HMM-GFP and ND-GFP cosedimented with actin filaments in the presence of ATP or in the presence of hexokinase and glucose to deplete ATP, whereas HMMΔN-GFP did not under the same conditions.

It has been well established that conventional myosin II and unconventional myosins cosediment with actin filaments in the absence of ATP to form a rigor complex (*13*, *21*−*25*). Unlike these myosins, HMMΔN-GFP, which contains a motor domain but not the N-terminal ATP-insensitive actin-binding site, did not cosediment with actin filaments even after depletion of ATP as shown above. This is another unique feature of this unusual myosin.

*Identification of the ATP-Insensitive Actin-Binding Site-(s) in the N-Terminal Domain.* The actin-binding site was located within the N-terminal domain, which is divided into three regions: the N-terminal region rich in K and E (residues 1−107), the C-terminal PDZ module (residues 217−344), and the middle region without any particular motif or characteristic sequences (residues 108−216). Hereafter, these three are designated as "KE", "PDZ", and "MIDDLE" regions. We searched for the ATP-insensitive actin-binding site in these regions using deletion constructs of the N-terminal domain. First, the KE region was deleted from the

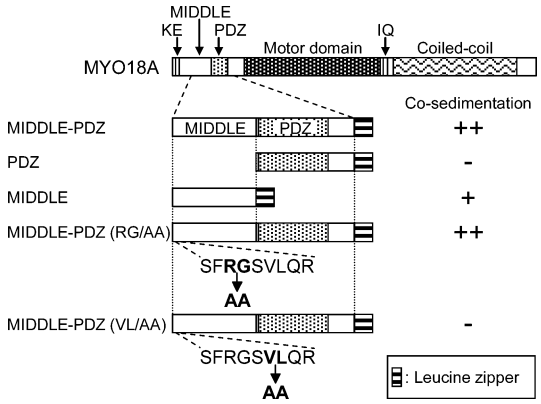


FIGURE 6: Schematic diagram of deletion constructs of the N-terminal domain expressed in *E. coli* strain BL21. For cosedimentation, ++, +, and − represent strong, positive, and no cosedimentation with actin filaments, respectively. KE stands for the KE rich region, MIDDLE for the MIDDLE region, PDZ for the PDZ module, and IQ for the IQ motif.

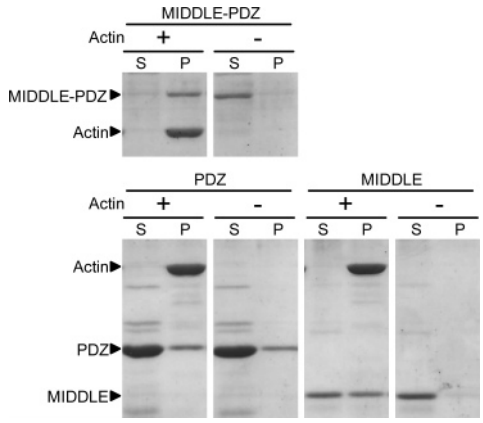


FIGURE 7: MIDDLE region (MIDDLE), but not the PDZ region (PDZ), of the N-terminal domain exhibits actin-binding activity. Bacterially expressed and purified deletion constructs of the N-terminal domain were centrifuged at 436000*g* with (+) or without (−) actin filaments. Resulting supernatants (S) and pellets (P) were subjected to SDS−PAGE and stained with Coomassie Brilliant Blue. The positions of each construct (MIDDLE-PDZ, PDZ, and MIDDLE) and actin on the gels are indicated. MIDDLE-PDZ and MIDDLE cosedimented with actin filaments, but PDZ did not.

N-terminal domain and the resulting MIDDLE-PDZ region was fused to the GCN4 leucine zipper for dimerization (Figure 6). The dimeric constructs were used here to mimic the dimeric structure of MYO18A. This bacterially expressed construct designated as MIDDLE-PDZ cosedimented with actin filaments (Figure 7), showing that the MIDDLE and/or PDZ regions contain the actin-binding site. Next, the dimeric deletion construct containing only the PDZ module (PDZ, Figure 6) was used for cosedimentation. This construct did not cosediment with actin filaments (Figure 7), suggesting that the actin-binding site is outside this PDZ module. The dimeric construct containing only the MIDDLE region without the PDZ module (MIDDLE, Figure 6) cosedimented with actin filaments (Figure 7), though the binding was weaker than that of the MIDDLE-PDZ fragment. Approximately half of the MIDDLE fragment remained in the supernatant even in the presence of an excess of actin filaments. This result implies either that the MIDDLE region primarily contributes to actin binding with a secondary, weak contribution of the PDZ module or that the truncation to generate the MIDDLE fragment affects its affinity with actin filaments.

The actin binding activity of the MIDDLE region was further confirmed by introducing point mutations to destroy the binding activity. To select targets for mutations, we compared the sequences of the N-terminal domains of MYO18A and -B, since it has recently been shown that the N-terminal domain of MYO18B alone exhibits colocalization with actin filaments in vivo when expressed as a GFP fusion protein (personal communication by J. Yukota and R. Ajima, National Cancer Center, Tokyo, Japan). As shown in Figure 8, there is a cluster of identical residues at the N-terminal end of the MIDDLE region of the two types of myosins. We targeted this cluster for mutations and made two mutants of the MIDDLE-PDZ construct in which R114 and G115 or V117 and L118 were mutated to alanine residues [MIDDLE-PDZ (RG/AA) and MIDDLE-PDZ (VL/AA), respectively (Figure 6)]. As shown in Figure 9, the former cosedimented with actin filaments, but the latter lost its binding activity. The R114 and G115 residues might be located on the surface of the MIDDLE region, while the V117 and L118 residues might be embedded inside as the hydrophobic core. Therefore, the latter mutations might affect the overall structure of the actin-binding site and be more effective in abolishing actin binding activity than the former. Although we cannot exclude the possibility that the effect of VL/AA mutations was not localized in the MIDDLE region due to propagation of structural changes, the results shown here collectively indicate that the MIDDLE region of the N-terminal domain (residues 108−216), which shows no homology to any actin-binding motifs or other functional module, contains the ATP-insensitive actin-binding site.

## DISCUSSION

This study identified an ATP-insensitive actin-binding site at the MIDDLE region of the N-terminal domain of MYO18A. This MIDDLE region does not contain any sequence homologous to the known actin-binding motifs. Monomeric unconventional myosins such as amoeboid myosin I have an ATP-insensitive actin-binding site, such as the GPA module in the tail domain (*26*). This type of myosin cross-links two actin filaments and generates sliding between them by anchoring itself on one filament through the ATP-insensitive actin-binding site in the tail and interact-

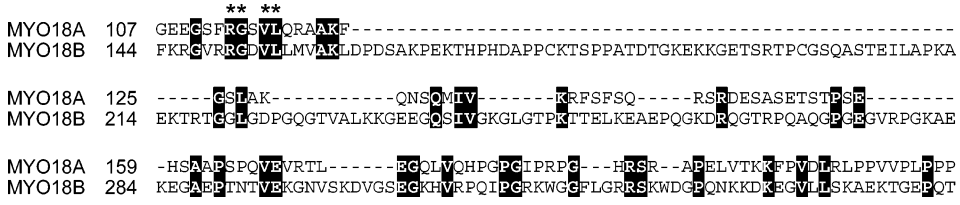


FIGURE 8: Amino acid sequence of the MIDDLE region of MYO18A compared with the corresponding region of MYO18B. Identical residues are highlighted in black. Residues mutated to alanine in MIDDLE-PDZ (RG/AA) or MIDDLE-PDZ (VL/AA) constructs are denoted with asterisks.

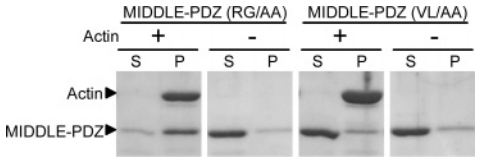


FIGURE 9: Point mutations in the MIDDLE region affect the actin binding activity of the MIDDLE-PDZ construct. Bacterially expressed and purified MIDDLE-PDZ constructs with point mutations at R114 and G115 [MIDDLE-PDZ (RG/AA)] or V117 and L118 [MIDDLE-PDZ (VL/AA)] were centrifuged at 436000*g* with (+) or without (−) actin filaments. Resulting supernatants (S) and pellets (P) were subjected to SDS−PAGE and stained with Coomassie Brilliant Blue. The positions of each construct [MIDDLE-PDZ (RG/AA) and MIDDLE-PDZ (VL/AA)] and actin on the gels are given. MIDDLE-PDZ (RG/AA) cosedimented with actin filaments, but MIDDLE-PDZ (VL/AA) did not.

ing with another filament through the motor domain in an ATP-dependent way. However, the two ATP-insensitive actin-binding sites in the dimeric MYO18A molecule stably cross-link actin filaments possibly for organizing a higher-order actin structure.

In this context, it must be noted that the colocalization of MYO18A with actin cytoskeletons is less striking for the full-length construct compared to the HMM-type construct lacking some of the tail domain. Thus, the deleted domain of MYO18A might regulate stable, ATP-insensitive cross-linking of actin filaments by the N-terminal domains. Proteins interacting with the PDZ module might also regulate actin cross-linking, although the binding partners of the PDZ module remain to be identified. Further studies are required to elucidate regulation of cross-linking of actin filaments by MYO18A.

Among members of the myosin superfamily, the myosin XVIII subfamily members have the most divergent sequences (*6*). The unusual sequences around the ATPase site of MYO18A, as described in the introductory section above, might affect its enzymatic behavior as a myosin. This notion is consistent with our observation that the motor domain of MYO18A did not cosediment with actin filaments even after depletion of ATP. The lack of the ability of the MYO18A motor domain to form a rigorlike complex with actin filaments and the presence of the two ATP-insensitive actin-binding sites at the N-terminal domains of the dimeric molecule collectively suggest that this unique myosin would not act as an active motor that slides along actin filaments. Instead, this myosin might stably cross-link actin filaments by the two ATP-insensitive actin-binding sites at the N-terminal domains for higher-order organization of the actin cytoskeleton.

After this paper had been submitted, similar results were reported by Mori et al. (*27*), who identified the actin-binding site at a region outside the PDZ module in the N-terminal domain of MYO18A by immunoprecipitation. In general, protein−protein interactions identified by immunoprecipitation could be mediated by a third protein. Our results reported here directly identified the stable actin-binding site by coprecipitation of purified fragments with actin filaments.

## ACKNOWLEDGMENT

We thank Dr. Jun Yokota and Dr. Rieko Ajima (National Cancer Center, Tokyo, Japan) for sharing their unpublished data of MYO18B.

## REFERENCES

1. Mermall, V., Post, P. L., and Mooseker, M. S. (1998) Unconventional myosins in cell movement, membrane traffic, and signal transduction, *Science 279*, 527−533.
2. Sellers, J. R. (2000) Myosins: A diverse superfamily, *Biochim. Biophys. Acta 1496*, 3−22.
3. Berg, J. S., Powell, B. C., and Cheney, R. E. (2001) A millennial myosin census, *Mol. Biol. Cell 12*, 780−794.
4. Furusawa, T., Ikawa, S., Yanai, N., and Obinata, M. (2000) Isolation of a novel PDZ-containing myosin from hematopoietic supportive bone marrow stromal cell lines, *Biochem. Biophys. Res. Commun. 270*, 67−75.
5. Mori, K., Furusawa, T., Okubo, T., Inoue, T., Ikawa, S., Yanai, N., Mori, K. J., and Obinata, M. (2003) Genome structure and differential expression of two isoforms of a novel PDZ-containing myosin (MysPDZ) (Myo18A), *J. Biochem. 133*, 405−413.
6. Yamashita, R. A., Sellers, J. R., and Anderson, J. B. (2000) Identification and analysis of the myosin superfamily in *Drosophila*: A database approach, *J. Muscle Res. Cell Motil. 21*, 491−505.
7. Tzolovsky, G., Millo, H., Pathirana, S., Wood, T., and Bownes, M. (2002) Identification and phylogenetic analysis of *Drosophila melanogaster* myosins, *Mol. Biol. Evol. 19*, 1041−1052.
8. Nishioka, M., Kohno, T., Tani, M., Yanaihara, N., Tomizawa, Y., Otsuka, A., Sasaki, S., Kobayashi, K., Niki, T., Maeshima, A., Sekido, Y., Minna, J. D., Sone, S., and Yokota, J. (2002) MYO18B, a candidate tumor suppressor gene at chromosome 22q12.1, deleted, mutated, and methylated in human lung cancer, *Proc. Natl. Acad. Sci. U.S.A. 99*, 12269−12274.
9. Smith, C. A., and Rayment, I. (1996) X-ray structure of the magnesium(II)·ADP·vanadate complex of the *Dictyostelium discoideum* myosin motor domain to 1.9 Å resolution, *Biochemistry 35*, 5404−5417.
10. Sasaki, N., Ohkura, R., and Sutoh, K. (2000) Insertion or deletion of a single residue in the strut sequence of *Dictyostelium* myosin II abolishes strong binding to actin, *J. Biol. Chem. 275*, 38705−38709.
11. O'Shea, E. K., Klemm, J. D., Kim, P. S., and Alber, T. (1991) X-ray structure of the GCN4 leucine zipper, a two-stranded, parallel coiled coil, *Science 254*, 539−544.
12. Spudich, J. A., and Watt, S. (1971) The regulation of rabbit skeletal muscle contraction. I. Biochemical studies of the interaction of the tropomyosin-troponin complex with actin and the proteolytic fragments of myosin, *J. Biol. Chem. 246*, 4866−4871.
13. Pollard, T. D., Stafford, W. F., and Porter, M. E. (1978) Characterization of a second myosin from *Acanthamoeba castellanii*, *J. Biol. Chem. 253*, 4798−4808.
14. Doberstein, S. K., and Pollard, T. D. (1992) Localization and specificity of the phospholipid and actin binding sites on the tail of Acanthamoeba myosin IC, *J. Cell Biol. 117*, 1241−1249.
15. Les Erickson, F., Corsa, A. C., Dose, A. C., and Burnside, B. (2003) Localization of a class III myosin to filopodia tips in transfected HeLa cells requires an actin-binding site in its tail domain, *Mol. Biol. Cell 14*, 4173−4180.
16. Reck-Peterson, S. L., Novick, P. J., and Mooseker, M. S. (1999) The tail of a yeast class V myosin, myo2p, functions as a localization domain, *Mol. Biol. Cell 10*, 1001−1017.
17. Buss, F., Arden, S. D., Lindsay, M., Luzio, J. P., and Kendrick-Jones, J. (2001) Myosin VI isoform localized to clathrin-coated vesicles with a role in clathrin-mediated endocytosis, *EMBO J. 20*, 3676−3684.
18. Zhang, H., Berg, J. S., Li, Z., Wang, Y., Lang, P., Sousa, A. D., Bhaskar, A., Cheney, R. E., and Stromblad, S. (2004) Myosin-X provides a motor-based link between integrins and the cytoskeleton, *Nat. Cell Biol. 6*, 523−531.
19. Kammerer, R. A., Schulthess, T., Landwehr, R., Lustig, A., Engel, J., Aebi, U., and Steinmetz, M. O. (1998) An autonomous folding unit mediates the assembly of two-stranded coiled coils, *Proc. Natl. Acad. Sci. U.S.A. 95*, 13419−13424.
20. Lister, I., Schmitz, S., Walker, M., Trinick, J., Buss, F., Veigel, C., and Kendrick-Jones, J. (2004) A monomeric myosin VI with a large working stroke, *EMBO J. 23*, 1729−1738.
21. Post, P. L., Bokoch, G. M., and Mooseker, M. S. (1998) Human myosin-IXb is a mechanochemically active motor and a GAP for rho, *J. Cell Sci. 111* (Part 7), 941−950.

22. Nascimento, A. A., Cheney, R. E., Tauhata, S. B., Larson, R. E., and Mooseker, M. S. (1996) Enzymatic characterization and functional domain mapping of brain myosin-V, *J. Biol. Chem. 271*, 17561−17569.
23. Hasson, T., and Mooseker, M. S. (1994) Porcine myosin-VI: Characterization of a new mammalian unconventional myosin, *J. Cell Biol. 127*, 425−440.
24. Komaba, S., Inoue, A., Maruta, S., Hosoya, H., and Ikebe, M. (2003) Determination of human myosin III as a motor protein having a protein kinase activity, *J. Biol. Chem. 278*, 21352−21360.
25. Berg, J. S., Derfler, B. H., Pennisi, C. M., Corey, D. P., and Cheney, R. E. (2000) Myosin-X, a novel myosin with pleckstrin homology domains, associates with regions of dynamic actin, *J. Cell Sci. 113* (Part 19), 3439−3451.
26. Rosenfeld, S. S., and Rener, B. (1994) The GPQ-rich segment of *Dictyostelium* myosin IB contains an actin binding site, *Biochemistry 33*, 2322−2328.
27. Mori, K., Matsuda, K., Furusawa, T., Kawata, M., Inoue, T., and Obinata, M. (2005) Subcellular localization and dynamics of MysPDZ (Myo18A) in live mammalian cells, *Biochem. Biophys. Res. Commun. 326*, 491−498.

BI0475931